Interfacial and optical properties of YO_xN_y gate dielectrics at different deposition temperatures

2009 J. Phys. D: Appl. Phys. 42 215405

(http://iopscience.iop.org/0022-3727/42/21/215405)

IOP PUBLISHING JOURNAL OF PHYSICS D: APPLIED PHYSICS

J. Phys. D: Appl. Phys. **42** (2009) 215405 (6pp) doi:10.1088/0022-3727/42/21/215405

Interfacial and optical properties of YO_xN_y gate dielectrics at different deposition temperatures

X J Wang[1,2], L D Zhang[1], G He[1], L Q Zhu[1], M Liu[1] and J P Zhang[1]

[1] Key Laboratory of Materials Physics, Anhui Key Laboratory of Nanomaterials and Nanostructure, Institute of Solid State Physics, Chinese Academy of Science, PO Box 1129, Hefei 230031, People's Republic of China

E-mail: xjwang2007@yahoo.com.cn

Received 4 January 2009, in final form 9 September 2009
Published 13 October 2009
Online at stacks.iop.org/JPhysD/42/215405

Abstract

YO_xN_y dielectric films were grown by rf-magnetron sputtering on a n-Si(1 0 0) substrate at different deposition temperatures from 300 to 550 °C. The interfacial properties of YO_xN_y films with different deposition temperatures were investigated using x-ray photoelectron spectroscopy and Fourier-transform infrared spectroscopy. It was found that an interfacial layer of yttrium silicate was formed between the YO_xN_y films and the Si substrate during deposition, and the higher the deposition temperature, the thicker the interfacial layer. The x-ray diffraction analysis shows that the phase transition of the YO_xN_y films occurs at substrate temperatures between 400 and 550 °C. The spectroscopic ellipsometry results indicate that the deposition temperature has a strong effect on the optical properties of the YO_xN_y films. The band gap was found to shift to higher energy at higher deposition temperature, which is likely due to the change in the crystalline structure of the YO_xN_y films.

1. Introduction

The demand for electronic devices with higher performance and lower consumption required a very aggressive reduction in the gate dielectric thickness in field-effect devices [1]. This rapid shrinking of the channel length and the gate dielectric thickness has forced the SiO_2 or its oxynitrides to meet its fundamental limits as conventional gate dielectrics because of significant leakage and reliability issues due to direct tunnelling, which is exponentially dependent on the dielectric thickness. Maintaining low tunnelling current requires an increase in the gate dielectric thickness and an accompanying increase in the dielectric constant (k), since capacitance scales as k/thickness, to obtain the desired equivalent silicon dioxide thickness (EOT). Therefore, a variety of metal oxides, including HfO_2, ZrO_2, Y_2O_3, TiO_2 and Al_2O_3, have been suggested as high-k replacements for silicon dioxide [2–6]. To apply these alternative gate dielectrics, a great challenge is their stability when in contact with the underlying silicon substrate [7]. A good interface that is thermodynamically stable and has a low density of states is essential in reducing the scattering effect on the charge carriers in the channel. Unfortunately most of these materials are not thermally stable if directly deposited onto a silicon substrate. SiO_2 or metal silicide often forms when they are deposited directly onto silicon or during subsequent annealing [8, 9]. Since SiO_2 or the metal silicide has a lower dielectric constant, even such a very thin layer of low-k material can reduce the capacitance of the stack and significantly degrade the electrical properties of the device. The N incorporation technology has shown to be advantageous in resolving this problem by inhibiting the interfacial reaction between gate dielectrics and the Si substrate [10, 11]. Niu *et al* [12] have reported that the rate of substrate oxidation slowed by the small amount of nitrogen in the Y_2O_3 film. Pan *et al* [13] have also found that the NH_3-nitrided layer is effective in minimizing interfacial YSi_xO_y formation by limiting the amount of Si available to interact with the Y_2O_3 layer. Moreover, the improved crystallization temperature and electrical performance of nitrogen-incorporated high-k films has also been reported [14, 15]. It is well known that the substrate temperature and post-deposition annealing have significant effects on the physical properties of thin

[2] Author to whom any correspondence should be addressed.

films [16–18]. However, the impact of substrate temperature on the interfacial and optical properties of the YO_xN_y films has not been reported in detail. In this paper, we investigated the interfacial properties of theYO_xN_y films at different deposition temperatures. Furthermore, the substrate temperature dependence of optical properties for theYO_xN_y films has also been discussed in detail.

2. Experimental details

The YO_xN_y films were deposited by reactive sputtering of Y target with purity of 99.99% in ambient $Ar/O_2/N_2$. The sputtering chamber was evacuated to 2.0×10^{-5} Pa before Ar and N_2 gases were introduced. The films were deposited onto n-type Si (1 0 0) single crystal substrates with resistivity of 4–12 Ω cm. Prior to deposition, the Si substrate was cleaned by Radio Corporation of America (RCA), followed by etching in 100 : 1 diluted HF solution, resulting in a hydrogen terminated surface. During deposition the total working pressure was maintained at approximately 1.0 Pa, while the rf power and substrate-to-target distance were kept at 100 W and 5.5 cm, respectively. In order to investigate the deposition-temperature dependence of interfacial and optical properties of the YO_xN_y films, deposition was performed at substrate temperatures of 300 °C, 400 °C and 550 °C, respectively.

X-ray photoelectron spectroscopy (XPS) and Fourier-transform infrared spectroscopy (FTIR) were used to investigate the interfacial properties of the YO_xN_y films. The XPS measurements were carried out using a VG ESCALAB 220i-XL system, equipped with a monochromatized Al *K*a source ($h\nu = 1486.6$ eV) for the excitation of photoelectrons. All the high-resolution scans were taken at a photoelectron take-off angle of 90° and a pass energy of 20 eV. The intensities for all the XPS spectra reported here have been normalized for comparison and all of the spectra are calibrated against the C 1s peak (285.0 eV) of adventitious carbon. A study of the interfacial properties of the YO_xN_y films was also carried out using FTIR. A Nicolet Magna-IR750 Fourier-transform infrared spectrometer was used. The resolution and number of scans were set at 4 cm^{-1} and 500, respectively. Film structure was analysed by x-ray diffraction (XRD) with a Cu Kα beam under an accelerated voltage of 40 kV and a current of 30 mA at a scan rate of 3 min^{-1}. An *ex situ* phase modulated spectroscopic ellipsometry (SE) was used to investigate the optical properties of the YO_xN_y films at different deposition temperatures in the spectral range 1.5–6.5 eV in steps of 50 meV at an incident angle of 70°.

3. Results and discussion

3.1. Interfacial properties and chemical structures of the YO_xN_y films

3.1.1. XPS studies. Figure 1(*a*) presents the Y3d photoelectron spectra for the YO_xN_y films with thicknesses of about 5 nm. It can be observed that the Y $3d_{2/5}$ peaks for all the films are shifted to higher energy than expected for Y $3d_{2/5}$ (156.8 eV) in Y_2O_3 [19], from 157.7 eV for the film deposited at 300 °C to 158.5 eV for the film deposited at 550 °C, indicating the formation of the silicate interfacial layer. According to previous report from Guittet [20], we believe that the shift of the Y $3d_{5/2}$ peak of the silicate interfacial layer to higher binding energy than that of Y_2O_3 is due to the fact that Y becomes more ionic in silicate than in Y_2O_3, and thus the bonds Y–O–Si involve a larger charge transfer than that in the Y–O bond. Figure 1(*b*) presents the Si 2p core level spectra, the peak located at 99.3 eV is due to the Si substrate and the higher binding energy peaks are assigned to the Si–O bonding in the Y–O–Si structure, which is lower than the expected binding energy for SiO_2 (103.3 eV) [19], but within the expected range for silicates (102–103 eV) [19]. The Y–O–Si peak shift from 103.0 eV for the film deposited at 300 °C to 102.4 eV for the film deposited at 550 °C and the intensity of the Y–O–Si peak increases with increasing deposition temperature, indicating the growth of the interfacial layer. It should be noted that no evidence for the Y–Si bond either as a low energy (<99.3 eV) feature on the silicon substrate peak or as a peak at 155.6 eV in the Y 3d spectrum, demonstrating no metal silicide formation during the YO_xN_y films deposition. The O 1s peak in figure 1(*c*) shifts from 530.2 eV for the film deposited at 300 °C to 531.8 eV for the film deposited at 550 °C, which also corresponds to Y silicates.

Figure 1(*d*) shows the N1s core level spectra of the YO_xN_y films. By using a curve-fitting method (nonlinear Gaussian lineshape fitting, the solid lines), the spectra can be deconvoluted into five components. The components with binding energies of 394 and 392 eV are assigned to Y 3s [19], the other three components with binding energies of 396.2 eV (N1), 398.8 eV (N2) and 402.2 eV (N3) are related to N chemical bonding. Based on the reported XPS results for SiON, the N2 component can be attributed to N species with three Si nearest neighbours ($N \equiv Si_3$) [21, 22]. On the other hand, the corresponding N1 peak at 396.8 eV is not related to the chemical bonds of Si–O–N compounds because the binding energy is lower than that for $N \equiv Si_3$. Considering the differential charging and extra-atomic relaxation effects [23, 24], we assigned N1 and N3 as N–Y and N–SiO_2, respectively. It can be observed that the intensity of N1 and N2 peaks increases with increasing deposition temperatures, which indicates the increase in nitrogen incorporation in the YO_xN_y films at higher deposition temperatures. This result is also confirmed by our previous work [25].

3.1.2. Fourier-transform infrared spectrometer studies. Figure 2 presents the mid-IR (1600–400 cm^{-1}) region of FTIR spectra in the transmission mode for the YO_xN_y films deposited at different temperatures. An absorption band around 1000 cm^{-1} is observed, which is related to the Si–O bonds in the Y–O–Si structure since the Si–O bonds in bulk SiO_2 is located at around 1080 cm^{-1} [26]. The band intensity increase as a function of deposition temperature demonstrates that the interfacial layer of the YO_xN_y films grows with increasing deposition temperature, which is consistent with the XPS results. It was reported that the growth of the interfacial layer during deposition or the post-annealing process in ambient O_2 gas is attributed mainly to the oxidation of the

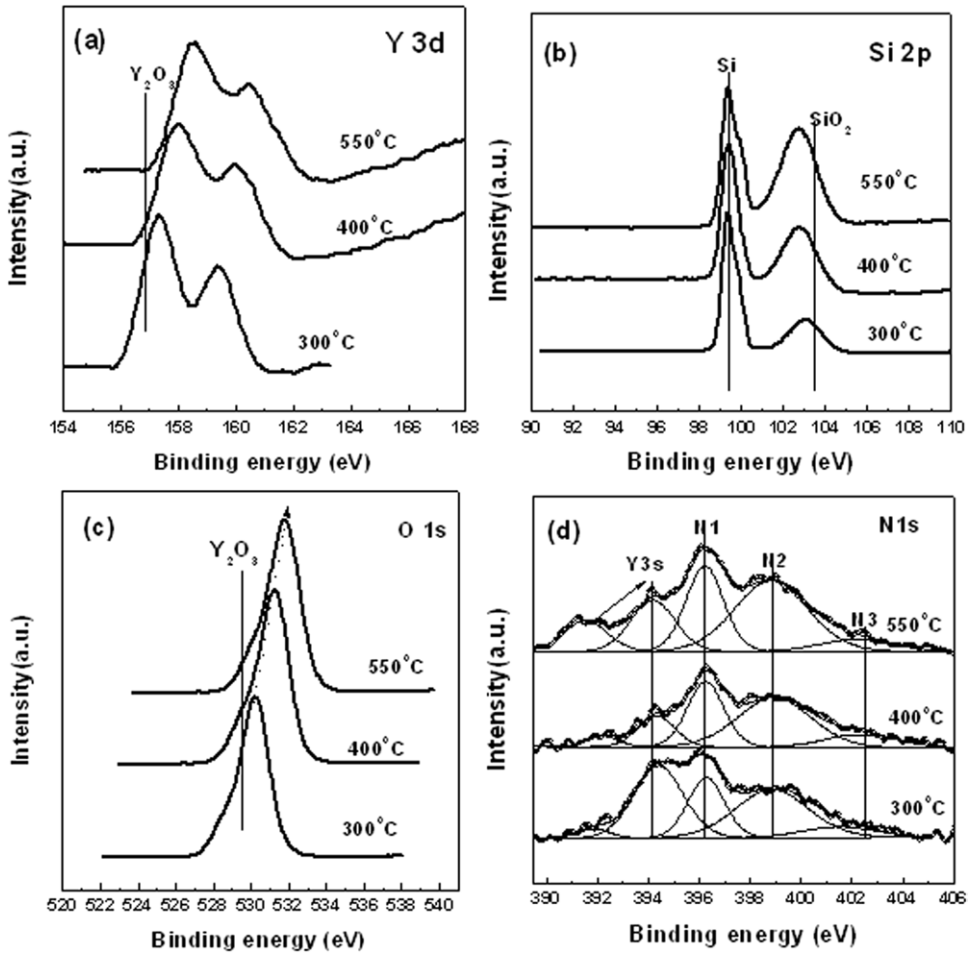

Figure 1. XPS spectra of YO_xN_y films deposited at different temperatures. (*a*) Y3d core level spectra, (*b*) Si 2p core level spectra, (*c*) O1s core level spectra and (*d*) N1s core level spectra.

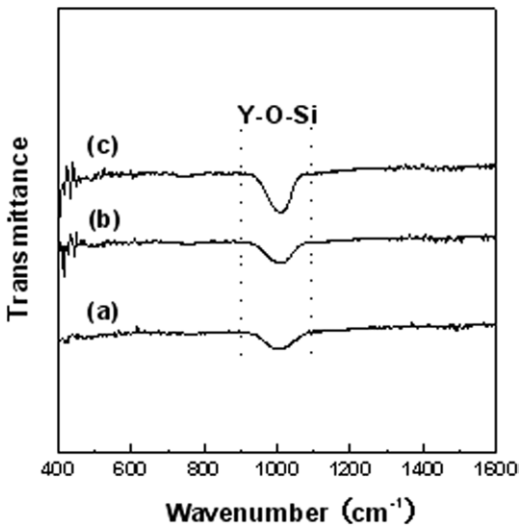

Figure 2. The deposition-temperature dependence of FTIR spectra for YO_xN_y films. (a) 300 °C, (b) 400 °C and (c) 550 °C.

silicon substrate by the diffusion of oxygen species through the Y_2O_3 films [27]. Two distinct issues need to be addressed to more fully understand interfacial reactions during high-*k* deposition: (1) SiO_2 formation at the silicon/dielectric interface and (2) reactions between the dielectric and the substrate that lead to mixed metal/oxygen/silicon (silicate) layers. The reaction scheme of elementary reactions for the formation of yttrium silicate can be written as follows:

$$Si + O_2 \rightarrow SiO_x, \quad (1)$$

$$SiO_x + YO_xNy + O_2 \rightarrow Y\text{–}O\text{–}N\text{–}Si. \quad (2)$$

3.2. The structure of the films

Figure 3 shows the crystalline structures of the YO_xN_y films deposited at various substrate temperatures. At 300 °C deposition, no peaks were observed in the XRD spectra, indicating that the YO_xN_y film is still amorphous. When the deposition temperature reaches 400 °C, a broad peak with $2\theta = 30.5^\circ$ was observed, which corresponds to the direction of the (0 0 3) plane of the monoclinic yttrium oxide phase. At 550 °C, the monoclinic structure abruptly disappears, and the typical diffraction peaks of the cubic Y_2O_3phase appear, suggesting the phase transition of the YO_xN_y films at substrate temperatures between 400 and 550 °C. This result is well consistent with the report from Cho *et al* [28]. The formation of the monoclinic structure of the YO_xN_y films at 400 °C deposition might depend on the formation path of the YO_xN_y

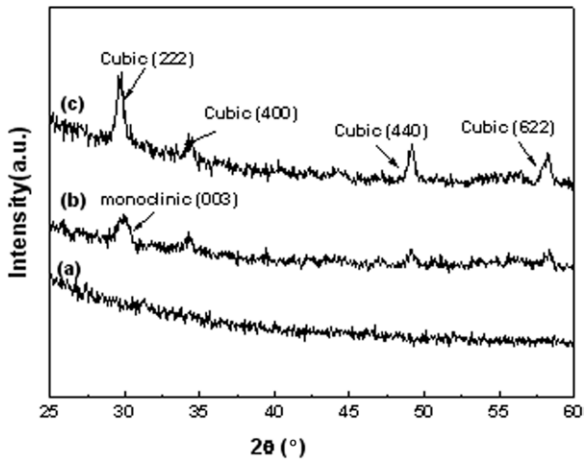

Figure 3. XRD pattern for YO_xN_y films deposited at different temperatures. (a) 300 °C, (b) 400 °C and (c) 550 °C.

structure. That is, at the low energy supplied, the monoclinic phase of the film is preferred because of the lower kinetic barrier compared with the cubic phase. As the substrate temperature reaches 550 °C, the energy is high enough to form the cubic phase, thus resulting in the phase transition of the YO_xN_y films.

3.3. Optical properties

We adopt the Tauc–Lorentz (TL) dispersion function [29] to characterize the optical properties of the YO_xN_y films. Essentially, the imaginary part (ε_2) of dielectric functions is obtained by combining the classical expression of the imaginary part of the dielectric functions above the band edge and the standard Lorentz expression, and the real part (ε_1) of dielectric functions is the result of self-consistent Kramers–Kronig integration of ε_2. The following equations summarize ε_1 and ε_2 as a function of photon energy E:

$$\varepsilon_2(E) = \begin{cases} \dfrac{AE_0C(E-E_g)^2}{(E^2-E_0^2)^2+C^2E^2}\cdot\dfrac{1}{E} & (E > E_g), \\ 0 & (E \leqslant E_g) \end{cases} \tag{3}$$

and

$$\varepsilon_1(E) = \varepsilon_\infty + \frac{2}{\pi}P\int_{E_g}^{\infty}\frac{\xi\varepsilon_2(\xi)}{\xi^2-E^2}\,\mathrm{d}\xi. \tag{4}$$

Equations (3) and (4) are uniquely defined by five parameters ε_∞, A (transition matrix element), C (broadening term), E_0 (peak transition energy) and E_g (optical band gap).

As is well known, the ellipsometric delta data are very sensitive to surface quality; thus it is very important to include surface roughness in all ellipsometric models to avoid non-physical absorption artefacts in the optical constants. The roughness was modelled as a mixture of 50% void and 50% bulk material using a Bruggeman effective medium approximation (BEMA) [30]. On the other hand, our XPS and FTIR results show that an interfacial layer exists between YO_xN_y films and Si substrates. Therefore, the four-phase model consisting of the substrate/interfacial layer/YO_xN_y film/surface rough layer was adopted to represent the films. For each sample, the five TL parameters and the film thickness

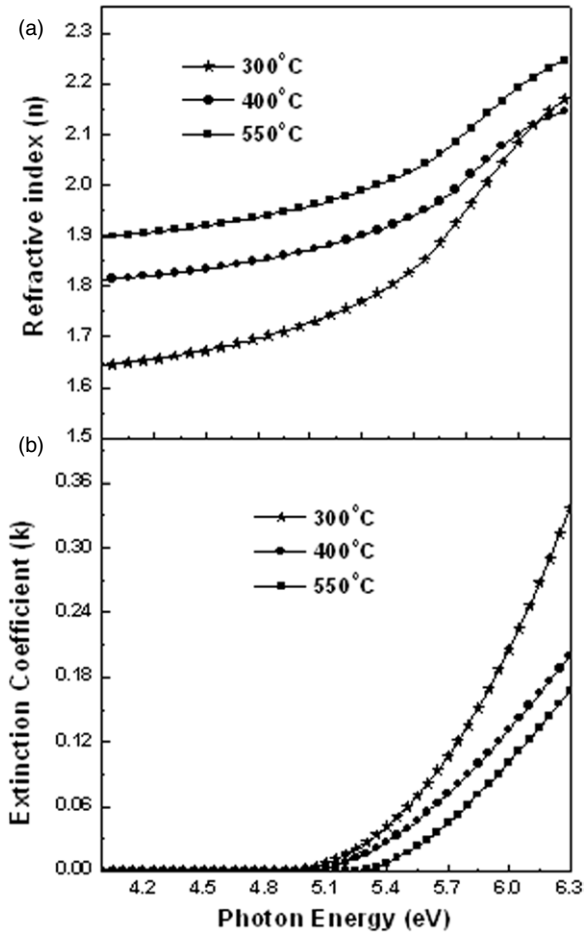

Figure 4. The deposition-temperature dependence of refractive index (n) and the extinction coefficient (k) of YO_xN_y films. (a) The refractive index (n) of YO_xN_y films. (b) The extinction coefficient (k) of YO_xN_y films.

are determined by least-squares fitting of their experimental data.

Figure 4(a) presents the deposition-temperature dependence of the refractive index (n) of the YO_xN_y films as determined by SE. It shows that n increases with increasing deposition temperatures. As is well known, the refractive index is closely related to the density and polarizability of the films [31]. Thus, the changes in density and/or polarizability would lead to a change in the refractive index. As our XPS result of the N1s core level spectra reveals that the amount of nitrogen incorporated into the films increases with increasing deposition temperatures, it is possible that the increase in nitrogen content results in the increase in refractive index since the metal–nitrogen bonds tend to be less polar than the corresponding metal–oxygen bonds, leading to a higher polarizability for the metal nitride [32]. Figure 4(b) shows the extinction coefficient (k) of theYO_xN_y films at different deposition temperatures. It is known that the extinction coefficient is related to the energy loss in the films, which is mainly caused by band-gap absorption in the absorption region. The decrease in the extinction coefficient with increasing deposition temperature, as shown in figure 4(b), suggests an increase in the band gap of the YO_xN_y films as will be discussed in detail below.

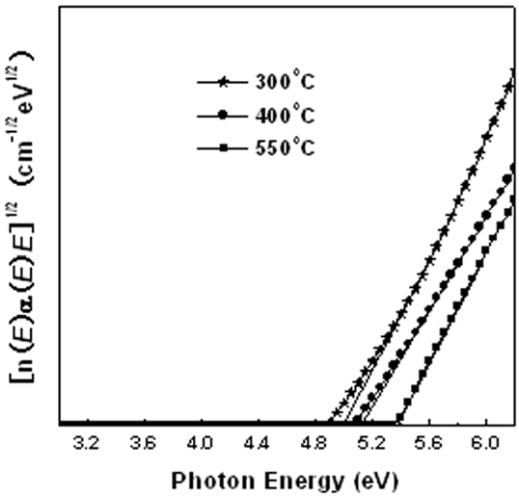

Figure 5. Tauc plots for determining the optical band gap E_g of YO_xN_y films at different deposition temperatures.

The method for determination of E_g is to use the Tauc plot [33]. Figure 5 presents the Tauc plots, as illustrated by the $[n(E)\alpha(E)E]^{1/2}$ versus photon energy (E). The band gap of the YO_xN_y films increases with an increase in deposition temperature, which corresponds to the increase in nitrogen content in the films, as shown in figure 1(*d*). This result seems contrary to our previous work [34], which reported that the band gap decreased with the increase in N content in the film. In this case, there might be two factors that influence the band gap of the YO_xN_y films. On the one hand, the increase in nitrogen content in the films with increasing deposition temperature might lead to the decrease in the band gap for the films. On the other hand, the crystalline structure also has a large effect on the band gap of oxides. Sayan *et al* [35] reported that the crystalline oxides have a larger band gap than amorphous oxides. Our XRD results (figure 3) show that as the deposition temperature increases, the crystalline degree of the films increases correspondingly, which would lead to the increase in the band gap for the YO_xN_y films. Based on the experimental data and the above analysis, it is obvious that the latter crystallization effect plays a dominant role in this case, resulting in a larger band gap at higher deposition temperature.

4. Conclusion

The interfacial properties, microstructure and optical properties of the YO_xN_y films deposited by rf-magnetron sputtering on the n-Si(1 0 0) substrate at different deposition temperatures were investigated. It was found that an interfacial layer of yttrium silicate was formed between the YO_xN_y films and the Si substrate during deposition, and the higher the deposition temperature, the thicker the interfacial layer. The phase transition of the YO_xN_y films occurs at substrate temperatures between 400 and 550 °C. The SE results indicate that the substrate temperature has a strong effect on the optical properties of the YO_xN_y films. The band gap was found to shift to higher energy at higher substrate temperature, which is likely due to the change in the crystalline structure of the YO_xN_y films.

Acknowledgment

This work was supported by the National Natural Science Foundation of China (Grant Nos 064N481507, 10804109 and 084NY11311-4)

References

[1] Gargini P 1999 *The International Technology Roadmap for Semiconductors* (Austin: S. I. Association)
[2] Wilk G D and Wallace R M 1999 *Appl. Phys. Lett.* **74** 2854
[3] Wilk G D and Wallace R M 2000 *Appl. Phys. Lett.* **76** 112
[4] Chambers J J and Parsons G N 2001 *J. Appl. Phys.* **90** 918
[5] Campbell S A, Gilmer D C, Wang X C, Hsieh M T, Kim H S, Gladfelter W L and Yan J 1997 *IEEE Trans. Electron Devices* **44** 104
[6] Manchanda L *et al* 1998 *Technical Digest Int. Electron Devices Meeting (Washington, DC)* p 605
[7] Wilk G D, Wallace R M and Anthony J M 2001 *J. Appl. Phys.* **89** 5243
[8] Lee B H, Kang L, Nieh R, Qi W J and Lee J C 2000 *Appl. Phys. Lett.* **76** 1926
[9] Jeon T S, White J M and Kwong D L 2001 *Appl. Phys. Lett.* **78** 368
[10] Chen P, Bhandari H B and Klein T M 2004 *Appl. Phys. Lett.* **85** 1574
[11] Quevedo-Lopez M A, El-Bouanani M, Kim M J, Gnade B E, Wallace R M, Visokay M R, Li-Fatou A, Bevan M J and Colombo L 2002 *Appl. Phys. Lett.* **81** 1609
[12] Niu D, Ashcraft R W, Hinkle C and Parsons G N 2004 *J. Vac. Sci. Technol.* A **22** 445
[13] Pan T M and Lee J D 2007 *J. Electrochem. Soc.* **154** H698
[14] Visokay M R, Chambers J J, Rotondaro A L P, Shanware A and Colombo L 2002 *Appl. Phys. Lett.* **80** 3183
[15] Alers G B, Fleming R M, Wong Y H, Dennis B, Pinczuk A, Redinbo G, Urdahl R, Ong E and Hasan Z 1998 *Appl. Phys. Lett.* **72** 1308
[16] Singh S, Ganguli T, Kumar R, Srinivasa R S and Major S S 2008 *Thin Solid Films* **517** 661
[17] Oh J H, Park Y, An K S, Kim Y, Ahn J R, Baik J Y and Park C Y 2005 *Appl. Phys. Lett.* **86** 262906
[18] Ioannou-Sougleridis V, Vellianitis G and Dimoulas A 2003 *J. Appl. Phys.* **93** 3982
[19] Moulder J F, Stickle W F, Sobol P E and Bomben K D 1992 *Handbook of X-ray Photoelectron Spectroscopy* (Eden Prairie: Perkin-Elmer Corporation)
[20] Guittet M J, Crocombette J P and Gautier-Soyer M 2001 *Phys. Rev.* B **63** 125117
[21] Lu Z H, Tay S P, Cao R and Pianetta P 1995 *Appl. Phys. Lett.* **67** 2836
[22] Rignanese G M, Pasquarello A, Charlier J C, Gonze X and Car R 1997 *Phys. Rev. Lett.* **79** 5174
[23] Iwata S and Ishizaka A 1996 *J. Appl. Phys.* **79** 6653
[24] Toyoda S, Okabayashi J, Kumigashira H, Oshima M, Liu G L, Liu Z, Ikeda K and Usuda K 2005 *Appl. Phys. Lett.* **87** 102901
[25] Zhu L Q, Fang Q, Wang X J, Zhang J P, Liu M, He G and Zhang L D 2008 *Appl. Surf. Sci.* **254** 5439
[26] Boyd I W and Wilson J I B 1987 *J. Appl. Phys.* **62** 3195
[27] Kang S K, Ko D H, Kim E H , Cho M H and Whang C N 1999 *Thin Solid Films* **353** 8
[28] Cho M H, Ko D H, Jeong K, Whangbo S W, Whang C N, Choi S C and Cho S J 1999 *Thin Solid Films* **349** 266
[29] Jellison G E and Modine F A 1996 *Appl. Phys. Lett.* **69** 371

[30] Aspnes D E, Theeten J B and Hottier F 1979 *Phys. Rev.* B **20** 3292
[31] Khawaja E E, Bouamrane F, Adel F A, Hallak B, Daous A and Salim A 1994 *Thin Solid Films* **240** 121
[32] Ohring M 1991 *The Materials Science of Thin Films* (San Diego, CA: Academic)
[33] Tauc J, Grigorovici R and Vancu A 1966 *Phys. Status Solidi* **15** 627
[34] Wang X J, Zhang L D, Liu M, Zhang J P and He G 2008 *Appl. Phys. Lett.* **92** 122901
[35] Sayan S *et al* 2005 *Appl. Phys. Lett.* **86** 152902